PHYSICAL REVIEW B **79**, 220401(R) (2009)

Unusual magnetic, thermal, and transport behavior of single-crystalline $EuRh_2As_2$

Yogesh Singh, Y. Lee, B. N. Harmon, and D. C. Johnston
Ames Laboratory and Department of Physics and Astronomy, Iowa State University, Ames, Iowa 50011, USA
(Received 13 May 2009; published 1 June 2009)

An *antiferromagnetic* transition is observed in single-crystal $EuRh_2As_2$ at a high temperature $T_N=47$ K compared to the *ferromagnetic* Weiss temperature $\theta=12$ K. We show that the large ratio $T_N/|\theta|\approx 4$ is, perhaps surprisingly, consistent with mean-field theory. A first-order field-induced magnetic transition is observed at $T<T_N$ with an unusual temperature dependence of the transition field. A dramatic magnetic field-induced reduction in the electronic specific heat coefficient at 1.8–5.0 K by 38% at 9 T is observed. In addition, a strong positive magnetoresistance and a large change in the Hall coefficient occur below 25 K. Band structure calculations indicate that the Fermi energy lies on a steep edge of a narrow peak in the density of states.

DOI: 10.1103/PhysRevB.79.220401 PACS number(s): 75.40.Cx, 71.20.Be, 75.30.Kz, 75.47.Np

The recent discovery of superconductivity with transition temperatures up to $T_c=38$ K in the layered iron arsenides AFe_2As_2 (A=Ba, Sr, Ca, and Eu) when the A atoms are partially replaced by K (Ref. 1) has led to a renewed interest in $ThCr_2Si_2$-structure materials. We have been carrying out a search for similar isostructural compounds such as $Ba(Rh,Mn)_2As_2$ (Ref. 2) in an attempt to significantly increase the maximum T_c for this class of compounds. We studied the physical properties of another member[3] of this structure class, $EuRh_2As_2$, and found a variety of novel behaviors as reported here.

Our primary results are as follows. First, from our anisotropic magnetic susceptibility χ versus temperature T data on $EuRh_2As_2$ single crystals, the Eu ions are found to have an intermediate valence 2.13(2) unusually close[4] to Eu^{+2}, which has a spin-only magnetic moment with $J=S=7/2$. Second, an unusually large *antiferromagnetic* (AFM) ordering temperature $T_N=47$ K compared to the *ferromagnetic* (FM) (positive) Weiss temperature $\theta\approx 12$ K is found. It is widely assumed that the magnitude of θ in the Curie-Weiss law $\chi=C/(T-\theta)$ is the mean-field transition temperature for either FM or AF ordering of a local moment system, which is the maximum transition temperature that the system can have. Magnetic fluctuations and frustration effects reduce the magnetic ordering temperature below the mean-field value, so our observation that $T_N/|\theta|\approx 4\gg 1$ is surprising. The resolution of this conundrum is simple: mean-field theory for a local moment antiferromagnet in fact *allows arbitrarily large values* of the ratio $T_N/|\theta|$.[5] This can happen in an antiferromagnet when FM exchange interactions between spins within the same sublattice exist, in addition to the usual AF interactions between spins on opposite sublattices.

Third, a very unusual and dramatic monotonic magnetic field-induced reduction in the electronic specific-heat coefficient γ is observed at 1.8–5.0 K by 38% at a relatively low field of 9 T. We suggest that field-induced stabilization[4] of the +2 valence of Eu is centrally involved. Finally, a strong positive magnetoresistance (MR) develops below 25 K that violates Kohler's rule, where $\rho(T)$ shows a "nonmetallic" increase with decreasing T at fixed H, together with a large change in the Hall coefficient below 25 K. These apparently coupled electronic behaviors have no obvious origin. Our band structure calculations indicate that the Fermi energy lies on a steep edge of a sharp peak in the density of states (DOS).

Single crystals of $EuRh_2As_2$ were grown out of Pb flux.[3] Single-crystal x-ray diffraction measurements confirmed that $EuRh_2As_2$ crystallizes in the tetragonal $ThCr_2Si_2$ structure with lattice parameters $a=4.075(4)$ Å and $c=11.295(2)$ Å at 298 K. The compositions of two crystals were determined using energy dispersive x-ray analysis, yielding the average atomic ratios Eu:Rh:As=20.8:37.9:41.3. The $\chi(T)$ and magnetization M versus applied magnetic field H isotherms were measured with a Quantum Design Magnetic Property Measurement System (MPMS) superconducting quantum interference device (SQUID) magnetometer. The $\rho(T)$, $C(T)$, and Hall effect were measured using a Quantum Design Physical Properties Measurement System (PPMS) instrument.

For the electronic DOS calculations, we used the full potential linearized augmented plane wave method with a local density approximation functional.[6] The difference in energy of 0.01 mRy/cell between successive iterations was used as a convergence criterion. The employed muffin tin radii are 2.5, 2.2, and 2.2 a.u. for Eu, Rh, and As, respectively. $4f$ electrons of Eu were treated as core electrons. The structural data were taken from Ref. 3. The total DOSs for both spin directions for $EuRh_2As_2$ and the partial DOS for Eu $5d$, Rh $4d$, and As $4p$ electrons versus the energy E relative to the Fermi energy E_F are shown in Fig. 1. E_F is located just below an extremely sharp peak in the DOS. The total DOS at E_F is $N(E_F)=3.38$ states/eV f.u. (f.u. means formula unit) for both spin directions with maximum contribution from the Rh $4d$ orbitals.

The $\chi(T)$ data for a crystal of $EuRh_2As_2$ measured with H parallel (χ_c) and perpendicular (χ_{ab}) to the c axis are shown in Fig. 2. The powder-averaged susceptibility $\chi_{\rm powder}=(2\chi_{ab}+\chi_c)/3$ is also shown in Fig. 2. The $\chi_{\rm powder}(T)$ data above 60 K were fitted by the expression $\chi(T)=f\chi_{Eu^{+3}}(T)+(1-f)C/(T-\theta)$, where the Van Vleck susceptibility $\chi_{Eu^{+3}}(T)$ of Eu^{+3} is given in Ref. 7, C is the Curie constant for Eu^{+2} with g-factor $g=2$,[8] and θ is the Weiss temperature for interactions between Eu^{+2} moments. An excellent fit was obtained with $f=0.13(2)$ and $\theta=12(2)$ K (inset). An average valence of 2.13(2) is therefore obtained for Eu. This is different from the value $\approx$2.00 obtained for $EuRh_2As_2$ in Ref.

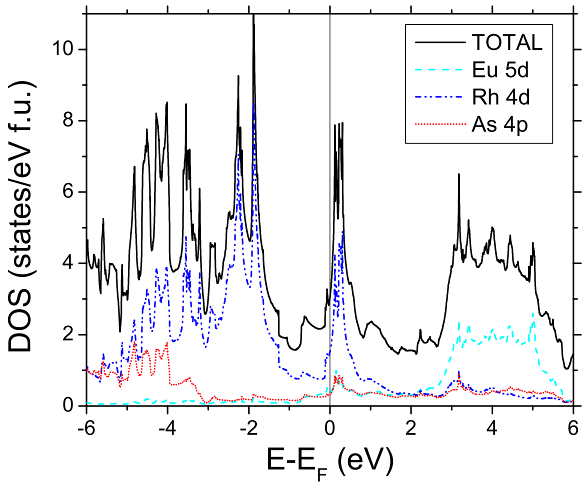

FIG. 1. (Color online) The DOS for $EuRh_2As_2$ versus energy E relative to the Fermi energy E_F and the partial DOS versus E from the Eu, Rh, and As atoms.

9, possibly due to composition differences of the samples.

The positive value $\theta = 12$ K indicates predominantly *ferromagnetic* exchange interactions between the magnetic Eu^{2+} moments. Surprisingly, however, in Fig. 2 we observe a sharp decrease in χ_{ab} indicating a transition into an *antiferromagnetic* state at a much *higher* Néel temperature $T_N = 47$ K. The χ_c also shows an abrupt change in slope at T_N and becomes weakly temperature dependent at lower T. The large value of $\chi_{ab}(T \to 0)$ indicates that $EuRh_2As_2$ is a noncollinear easy-plane antiferromagnet with the easy plane being the *ab* plane. Magnetic x-ray scattering measurements on our crystals at $H=0$ revealed both commensurate and incommensurate magnetic structures in which the Eu spins are ferromagnetically aligned within the *ab* plane and where the spins in adjacent planes are, or are nearly, antiparallel.[10]

A large ratio of $T_N/|\theta|$ can occur within mean-field theory for a two-sublattice collinear antiferromagnet with equal numbers of spins on the two sublattices, each with Curie constant $C/2$, as follows. A spin in each sublattice is assumed to interact with the same number of spins both within

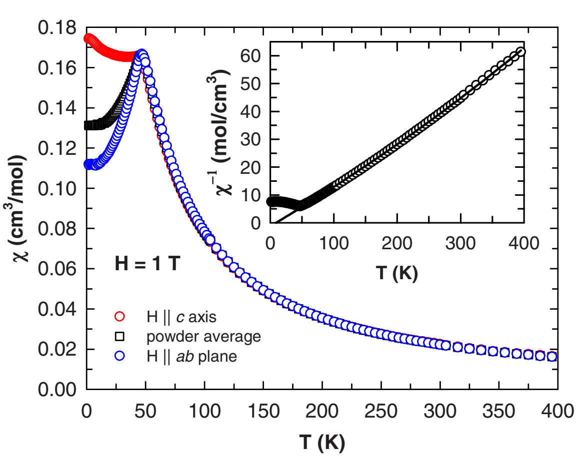

FIG. 2. (Color online) χ_{ab} and χ_c versus temperature T for $EuRh_2As_2$. The powder-averaged $\chi_{\rm powder}$ is also shown. Inset: fit (solid curve) of the $\chi^{-1}(T)$ data (open circles) (see text).

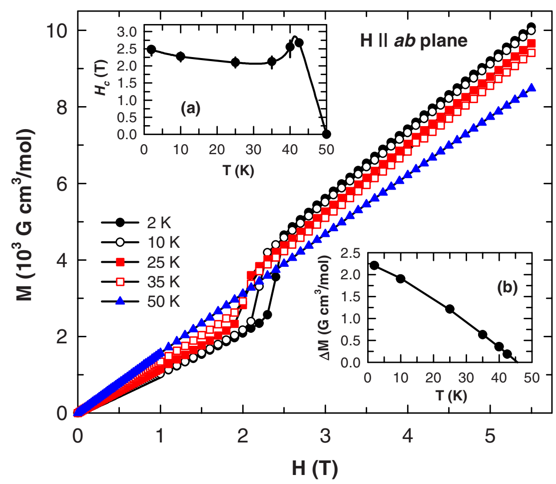

FIG. 3. (Color online) $M(H)$ at various T with H applied parallel to the *ab* plane. Inset (a): metamagnetic field H_c versus T. The vertical bars on the data points are the widths of the metamagnetic transition. The solid curve is a guide to the eyes. Inset (b): change in magnetization ΔM at the transition versus T.

its own sublattice and with the other sublattice with mean-field coupling constants λ_1 and λ_2, respectively. Applying the usual mean-field treatment one obtains the Weiss temperature $\theta = C(\lambda_1 + \lambda_2)/2$ and magnetic ordering temperature $T_N = C(\lambda_1 - \lambda_2)/2$. Thus,

$$\frac{T_N}{\theta} = \frac{\lambda_1 - \lambda_2}{\lambda_1 + \lambda_2} = \frac{\mathcal{J}_1 - \mathcal{J}_2}{\mathcal{J}_1 + \mathcal{J}_2}, \tag{1}$$

where $\mathcal{J}_1$ and $\mathcal{J}_2$ are the nearest-neighbor exchange coupling constants for two spins in the same and different sublattices, respectively. If $\lambda_1, \mathcal{J}_1 > 0$ (FM), and $\lambda_2, \mathcal{J}_2 < 0$ (AF) one can obtain arbitrarily large values of the ratio $T_N/|\theta|$. For our case with $T_N/\theta \approx 4$, Eq. (1) yields $\lambda_1/\lambda_2 = \mathcal{J}_1/\mathcal{J}_2 \approx -5/3$.

$M(H)$ isotherms at various T with H applied along the *ab* plane are shown in Fig. 3. The $M(H)$ data for $H \| c$ (not shown) are proportional at all temperatures from 2 to 300 K. The $M(H)$ data for H applied along the *ab* plane are also proportional for temperatures $T > T_N = 47$ K as seen in Fig. 3. However, for $T < T_N$ the $M(H)$ is initially proportional but then shows a first-order steplike increase in M at a metamagnetic critical field H_c which exhibits hysteresis (not shown) upon increasing and decreasing H. Above H_c, M again is proportional to H but with a larger slope. The value of M at $T = 2$ K and $H = 5.5$ T is only 1.81 μ_B/f.u., which is much smaller than the expected Eu^{2+} saturation moment of 7.0 μ_B/Eu. Our data thus indicate that a first-order transition between two antiferromagnetically ordered states occurs at H_c. Figure 3 inset (a) shows that H_c decreases initially with increasing T between 2 and 25 K, as expected, but then increases strongly upon further approaching T_N. At $T = 50$ K $> T_N$ we did not observe any metamagnetic transition. The increase in magnetization ΔM across the metamagnetic transition versus T is shown in Fig. 3 inset (b). In contrast to H_c, ΔM shows a monotonic decrease in T and vanishes near T_N as expected.

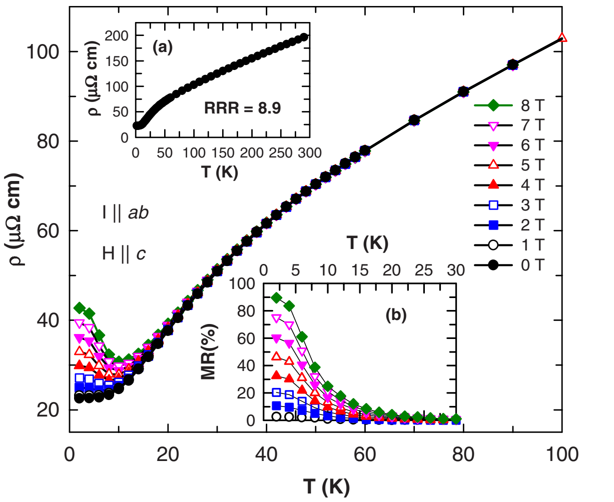

FIG. 4. (Color online) Resistivity ρ in the *ab* plane versus temperature T measured in various $H \| c$. Inset (a): $\rho(T)$ for $H=0$. Inset (b): MR below $T=30$ K.

The $\rho(T)$ data for current in the *ab* plane for $H=0$ and for temperatures from 2 to 300 K are shown in Fig. 4 inset (a). These data indicate metallic behavior with a residual resistivity ratio (RRR)$=\rho(300\text{ K})/\rho(2\text{ K})=8.9$. There is no sudden reduction in $\rho(T)$ below $T_N=47$ K as might be expected below a magnetic ordering transition due to a reduction in spin-disorder scattering. This is particularly surprising in view of the sharp transitions at T_N seen in $\chi(T)$ and $C(T)$ in Figs. 2 and 6 below, respectively.

The field-dependent $\rho(T,H)$ data are shown in Fig. 4 between 2 and 100 K. A strong increase in ρ occurs with increasing H beginning below 25 K. The magnetoresistance percentage values $\text{MR}(H,T) \equiv 100[\rho(H,T)-\rho(0,T)]/\rho(0,T)$ versus T at various H are shown in Fig. 4 inset (b). A large MR is seen at low T with increasing H: the MR reaches 90% at $T=2$ K and $H=8$ T. From the single-band relation $\omega_c\tau = |R_H|H/\rho$, where ω_c is the cyclotron frequency, τ is the mean-free scattering time of the current carriers and R_H is the Hall coefficient, and using our experimental R_H (below) and ρ data at 2 K, one finds that our MR data are in the low-field regime $\omega_c\tau \sim 0.003 \ll 1$ at 8 T. In this regime one normally expects[11] MR $\sim H^2$ instead of the different behavior we observe in Fig. 5 inset. A positive MR can occur due to increased spin-disorder scattering upon suppression of an antiferromagnetic ordering by a magnetic field.[12] However, this explanation is untenable here because as shown in Fig. 6 below, the T_N of $EuRh_2As_2$ is suppressed to only ~ 40 K in $H=8$ T. Furthermore, one expects a zero MR with $H \| c$ ($H \perp$ ordered moment direction) due to AF fluctuations at $T \ll T_N$.[13] According to semiclassical transport theory, the MR follows Kohler's rule $\text{MR}=F[H/\rho(0)]$, where $F(x)$ is a universal function for a given material, if there is a single species of charge carrier and the scattering time is the same at all points on the Fermi surface.[11] As shown in Fig. 5 inset, the MR in $EuRh_2As_2$ severely violates Kohler's rule.

The Hall coefficient R_H was found to be independent of H up to 8 T and is plotted versus T at $H=8$ T in Fig. 5. R_H is negative and increases slowly with decreasing T from 200 to 25 K but then increases rapidly below 25 K, the temperature

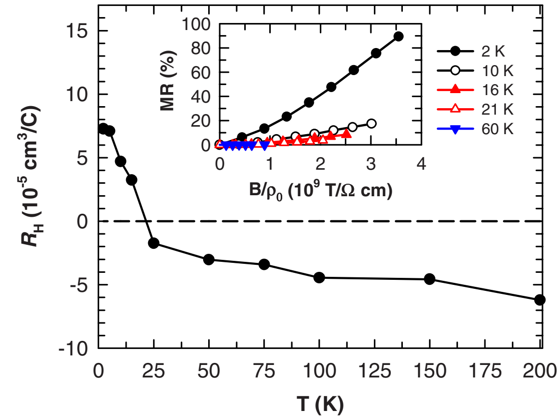

FIG. 5. (Color online) Hall coefficient R_H vs T for $EuRh_2As_2$. Inset: MR versus $H/\rho(H=0)$ at various T.

below which the MR also begins to strongly increase. An unusual T dependence of R_H is sometimes seen across a magnetic transition.[14] However, the strong increase in R_H for $EuRh_2As_2$ occurs below 25 K which is well below $T_N(H)$ as shown next.

The $C(T)$ of a single crystal of $EuRh_2As_2$ measured between 1.8 and 70 K in various $H \| c$ is shown in Fig. 6. For $H=0$, a second-order anomaly with an onset at 48.3 K and a peak at 44.3 K is observed from which we estimate $T_N \approx 46$ K in agreement with the T_N found from our $\chi(T)$ data above. The $C(T)$ data for a single crystal of $BaRh_2As_2$,[2] also shown in Fig. 6, were used to estimate the lattice heat capacity of $EuRh_2As_2$. Figure 6 inset (a) shows $\Delta C(T)$ versus T between 2 and 100 K, obtained by subtracting the heat capacity of $BaRh_2As_2$, adjusted for the molar mass difference with $EuRh_2As_2$, from that of $EuRh_2As_2$. $\Delta C(T)$ is consistent with a mean-field transition at T_N as follows. In mean-field theory, the magnitude of the heat capacity jump at T_N is given by $\Delta C(T_N)=\frac{5}{2}R\frac{(2S+1)^2-1}{(2S+1)^2+1}=16.2$ J/mol K^2 for $S=7/2$,[15]

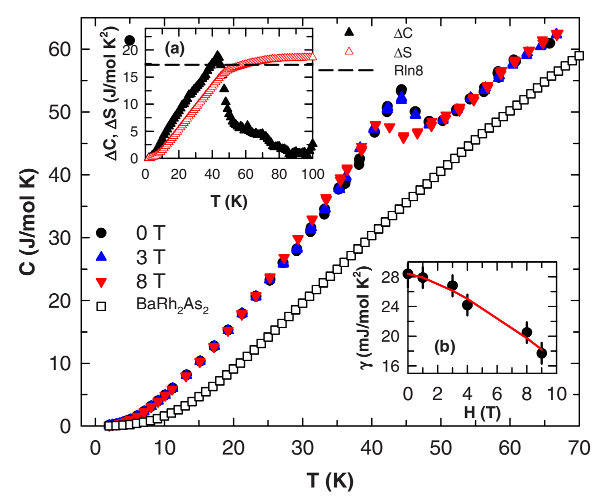

FIG. 6. (Color online) Heat capacity C vs T of single-crystal $EuRh_2As_2$ at various $H \| c$ and for single-crystal $BaRh_2As_2$ in $H=0$. Inset (a): $\Delta C(T)$ and $\Delta S(T)$ vs T. The dashed horizontal line is the value $\Delta S=R\ln 8$ expected for disordered Eu^{2+} ($J=S=7/2$) spins. Inset (b): γ versus H.

where R is the gas constant. This value is close to that observed in Fig. 6 inset (a). Furthermore, the entropy difference $\Delta S(T)$ versus T obtained by integrating the $\Delta C(H=0,T)/T$ versus T, as shown in Fig. 6 inset (a), reaches the value $R \ln 8$ expected for Eu^{2+} moments ($J=S=7/2$) just above T_N after which it becomes nearly T independent. From the $C(T,H)$ data, one sees that T_N decreases by only ~5 K at 8 T. Thus we infer that the strong positive MR below ~25 K in Fig. 4 does not result from suppression of T_N to these low temperatures.

At 1.8–5.0 K, the heat capacity of $EuRh_2As_2$ obeys $C(T,H)=\gamma(H)T+\beta T^3$, where $\beta \approx 7.1(1)$ mJ/mol K^4 is independent of H and the electronic specific-heat coefficient $\gamma(H)$ is plotted in Fig. 6 inset (b). Between $H=0$ and 9 T, γ decreases monotonically from 28.4(9) to 17.7(7) mJ/mol K^2, a remarkable reduction of 38%. This reduction in γ might be explained by a field-induced carrier localization; however, the field independence of R_H (above) argues against such an interpretation. From $N(E_F)=3.38$ states/eV f.u. obtained above from our band structure calculations for a valence Eu^{+2}, we obtain $\gamma=7.96$ mJ/mol K^2 assuming zero electron-phonon coupling. This value is about 3.5 times smaller than the observed zero-field value. This discrepancy suggests that the high observed $\gamma(H=0)$ is due to the intermediate valence 2.13(2) of Eu inferred from $\chi(T)$ above T_N (Ref. 16) and that the field-induced reduction in γ toward the band structure value arises from field-induced stabilization[4] of the Eu valence toward Eu^{+2} and concomitant reduction in the spin fluctuation[16] contribution.

In summary, our magnetic, transport, and thermal measurements on single crystals of $EuRh_2As_2$ revealed an array of interesting and unusual behaviors. From $\chi(T)$ measurements at temperatures $T>T_N$, the Eu ions are found to have an intermediate valence 2.13(2) unusually close[4] to Eu^{+2}. The large ratio $T_N/\theta \approx 4$ is very unusual. A simple two-sublattice mean-field model where each sublattice interacts with itself in addition to the other explains how $T_N/|\theta|>1$ can come about. Other relevant examples of antiferromagnets where $T_N/|\theta|>1$ have been reported,[5,17–19] although the authors did not take specific note of this ratio. For $LaMnO_3$, using Eq. (1) and the $\mathcal{J}_{1,2}$ values in Ref. 20, one obtains the mean-field ratio $T_N/\theta=3.8$, slightly larger (as expected) than the observed value of 3.0 obtained from $\theta=46$ K and $T_N=140$ K.[19] In retrospect, it is surprising that antiferromagnets with $T_N/|\theta|>1$ are not more commonly observed. The temperature variation in the metamagnetic field H_c as T_N is approached is anomalous. The strong decrease in the electronic heat capacity coefficient γ with H at relatively low fields up to 9 T is very unusual.[21] In most metals, γ is independent of H in such fields because the magnetic field energy of a conduction carrier is far smaller than the Fermi energy. We suggest that the observed $\gamma(H)$ results from a field-induced stabilization[4] of the Eu valence toward Eu^{+2} at low T. This hypothesis can be checked using, e.g., x-ray absorption spectroscopy.[4] A strong positive magnetoresistance and a strong increase in R_H develop below 25 K suggesting a possible temperature-induced redistribution of carriers between electronlike and holelike Fermi surfaces, which can be tested using angular-resolved photoemission spectroscopy.

We thank S. Nandi, A. Kreyssig, A. I. Goldman, and J. Schmalian for helpful discussions and A. Ellern for structure analysis. Work at Ames Laboratory was supported by the Department of Energy, Basic Energy Sciences under Contract No. DE-AC02-07CH11358.

[1] For a review, see M. V. Sadovskii, Usp. Fiz. Nauk **51**, 1201 (2008).

[2] Yogesh Singh, Y. Lee, S. Nandi, A. Kreyssig, A. Ellern, S. Das, R. Nath, B. N. Harmon, A. I. Goldman, and D. C. Johnston, Phys. Rev. B **78**, 104512 (2008); Yogesh Singh, A. Ellern, and D. C. Johnston, *ibid.* **79**, 094519 (2009).

[3] A. Hellmann, A. Loehken, A. Wurth, and A. Mewis, Z. Naturforsch., B: Chem. Sci. **62**, 155 (2007).

[4] Y. H. Matsuda, T. Inami, K. Ohwada, Y. Murata, H. Nojiri, Y. Murakami, A. Mitsuda, H. Wada, H. Miyazaki, and I. Harada, J. Phys. Soc. Jpn. **77**, 054713 (2008).

[5] For simplicity and clarity, here we only consider Heisenberg spin interactions and exclude cases where θ arises from, or is affected by, single-ion effects.

[6] J. P. Perdew and Y. Wang, Phys. Rev. B **45**, 13244 (1992).

[7] J. H. Van Vleck, *The Theory of Electric and Magnetic Susceptibilities* (Clarendon, Oxford, 1932), p. 248.

[8] R. H. Taylor and B. R. Coles, J. Phys. F: Met. Phys. **5**, 121 (1975).

[9] G. Michels, M. Roepke, T. Niemöller, M. Chefki, M. M. Abd-Elmeguid, H. Micklitz, E. Holland-Moritz, W. Schlabitz, C. Huhnt, B. Büchner, A. Wurth, A. Mewis, and V. Kataev, J. Phys.: Condens. Matter **8**, 4055 (1996).

[10] S. Nandi, A. Kreyssig, Y. Lee, Yogesh Singh, J. W. Kim, D. C. Johnston, B. N. Harmon, and A. I. Goldman, Phys. Rev B **79**, 100407(R) (2009).

[11] A. B. Pippard, *Magnetoresistance in Metals*, 1st ed. (Cambridge University Press, Cambridge, 1989).

[12] Z. Ren, Z. Zhu, S. Jiang, X. Xu, Q. Tao, C. Wang, C. Feng, G. Cao, and Z. Xu, Phys. Rev. B **78**, 052501 (2008).

[13] H. Yamada and S. Takada, J. Phys. Soc. Jpn. **34**, 51 (1973).

[14] C. M. Hurd, *The Hall Effect in Metals and Alloys* (Plenum Press, New York, 1972).

[15] J. S. Smart, *Effective Field Theories of Magnetism* (W. B. Saunders Company, Philadelphia, 1966).

[16] C. M. Varma, Rev. Mod. Phys. **48**, 219 (1976).

[17] E. M. Levin, K. A. Gschneidner, Jr., T. A. Lograsso, D. L. Schlagel, and V. K. Pecharsky, Phys. Rev. B **69**, 144428 (2004).

[18] S. L. Bud'ko, Z. Islam, T. A. Wiener, I. R. Fisher, A. H. Lacerda, and P. C. Canfield, J. Magn. Magn. Mater. **205**, 53 (1999).

[19] C. Ritter, M. R. Ibarra, J. M. De Teresa, P. A. Algarabel, C. Marquina, J. Blasco, J. Garcia, S. Oseroff, and S. W. Cheong, Phys. Rev. B **56**, 8902 (1997).

[20] R. J. McQueeney, J.-Q. Yan, S. Chang, and J. Ma, Phys. Rev. B **78**, 184417 (2008).

[21] See also Y. Aoki, T. Fukuhara, H. Sugawara, and H. Sato, J. Phys. Soc. Jpn. **65**, 1005 (1996).